Polymer 51 (2010) 308–315

Contents lists available at ScienceDirect

Polymer

journal homepage: www.elsevier.com/locate/polymer

Electronic characterization of all-thiophene conducting dendrimers: Molecules and assemblies

Francisco Rodríguez-Ropero [a,*], David Zanuy [a,*], Carlos Alemán [a,b,*]

[a] Departament d'Enginyeria Química, E. T. S. d'Enginyeria Industrial de Barcelona, Universitat Politècnica de Catalunya, Diagonal 647, 08028 Barcelona, Spain
[b] Center for Research in Nano-Engineering, Universitat Politècnica de Catalunya, Campus Sud, Edifici C', C/Pasqual i Vila s/n, Barcelona E-08028, Spain

ARTICLE INFO

Article history:
Received 29 September 2009
Accepted 2 November 2009
Available online 10 November 2009

Keywords:
Dendrimers
Conducting materials
Electronic structure

ABSTRACT

The molecular and electronic structure of all-thiophene dendrimers in both the neutral and oxidized states have been investigated performing quantum mechanical calculations on systems of up to 30 rings. Results evidenced that the repulsive steric interactions between the neighboring thiophene rings induce significant distortions from the planarity independently of the electronic state. On the other hand, the ionization potential per thiophene ring and the lowest π–π^* transition energy decreases with the inverse of the longest α-conjugated chain of the dendrimer, *i.e.* when the generation increases. The lowest π–π^* transition energy predicted for an infinite generation dendrimer is 2.08 eV indicating that these materials are potential candidates to be used in optoelectronics. Additionally, Quantum mechanics/molecular mechanics calculations have been performed considering both the sandwich and T-shaped supramolecular arrangements. Results showed not only the stability of these aggregates but also the significant influence of the intermolecular electronic delocalization in the electronic properties of these materials.

1. Introduction

Over the past decades the interest towards conducting polymers has attracted the attention of many researchers because of their wide range of technological applications in fields such as electronics, biomedical engineering or optics [1]. Among conducting polymers, materials based on thiophene have settled as a prominent family because of the high stability of their doped and undoped states, the easiness to tune their structure and their controllable electrochemical behavior, giving rise to diverse applications in the areas of microelectronics, electrode materials, optoelectronics and sensors [2]. Electronic conduction in polythiophene derivatives is founded on their characteristic polyconjugated nature, which promotes both the intramolecular and intermolecular delocalization of π-electrons [3]. Although the synthesis and investigation of a number of conventional thiophene derivatives have been vastly exploited in the last decade [4], investigation on all-thiophene based dendrimers is currently one of the most challenging achievements [5–9].

Dendrimers are ideally perfect monodisperse macromolecules composed by a multifunctional core unit where a defined number of units called *dendrons* are attached leading to a regular and highly branched three-dimensional architecture. Three topological regions coexist in dendrimers, *i.e.* the inner dense core, the dendritic region around the core and the external surface, being the number of repeating units between the inner core and a terminal unit defined as *dendron generation* [10]. The peculiar architecture of dendrimers and the possibility of easily tuning their surface by adding different functional groups make them attractive materials to be used in a great variety of fields such as in biomedical applications [11], catalysis [12], sensing [13], or optoelectronics [14]. In the latter field the electronic properties of conducting polymers combined with both the great shape stability and the ability to self-assemble of dendrimers [15], offer new possibilities for designing new optoelectronic devices [16].

Given the aforementioned assumptions, all-thiophene based dendrimers are considered as a very promising kind of conducting material. They were synthesized and characterized for the first time by Advincula and co-workers [5]. Specifically, these researchers prepared a series of *n*T dendrimers, where *n* refers to the number of thiophene rings (T), with $n = 3$, 6, 7, 14, 15 and 30 using metal-mediated coupling reactions through a convergent approach. The potential use of such dendrimers in optoelectronics and molecular electronics was evidenced by their very broad absorption spectra and the ability of the bigger dendrimers to self-assemble on different

* Corresponding authors. Departament d'Enginyeria Química, E. T. S. d'Enginyeria Industrial de Barcelona, Universitat Politècnica de Catalunya, Diagonal 647, 08028 Barcelona, Spain. Tel.: +34 93 401 08 83; fax: +34 93 401 71 50.
E-mail addresses: francisco.rodriguez-ropero@upc.edu (F. Rodríguez-Ropero), david.zanuy@upc.edu (D. Zanuy), carlos.aleman@upc.edu (C. Alemán).

0032-3861/$ – see front matter © 2009 Elsevier Ltd. All rights reserved.
doi:10.1016/j.polymer.2009.11.007

solid substrates forming nanowires and 2-D crystalline structures. On the other hand, Bäuerle and co-workers [6] synthesized different all-thiophene dendrimers containing up to 90 thiophene rings (90T) with a divergent/convergent approach to facilitate the inclusion of functionalities in the external surface of the conducting dendrimer. More recently, femtosecond transient absorption measurements showed the suitability of all-thiophene dendrimers as light harvesting antennae for solar cells devices [7]. Concerning their optical properties, non-linear optical and excited state dynamical investigations evidenced a delocalization of the excitation throughout all the thiophene units and ultrafast energy transfer to the longest branch of the dendrimer [7]. Moreover, all-thiophene dendrimers have been demonstrated to be good sensors for entangled photons at very low flux making them suitable materials for imaging of biological systems, quantum optical applications and remote sensing [9].

Given the importance of the electronic properties in the applications of all-thiophene dendrimers, theoretical studies based on quantum mechanics (QM) are necessary not only to provide comprehensive understanding at the microscopic level but also to gain deeper insight on the intrinsic characteristics of these materials. In this article we use QM methods to study the structural and electronic properties of *n*T dendrimers with $n = 3$, 7, 14, 15 and 30 (Scheme 1). Since the electrical properties of poly(thiophene) derivatives are promoted by p-doping, *i.e.* an oxidation process [17], QM calculations have been performed considering both the neutral and the oxidized states of the dendrimers under study. Special attention has been paid to the evaluation of the lowest π–π^* transition energy, which has been determined using not only a conventional QM method but also a sophisticated time-dependent approach. Furthermore, calculations based on a theoretical procedure that combines quantum mechanics and molecular mechanics (QM/MM calculations) have been used to examine the supramolecular assembly of the 30T dendrimer.

2. Methods

2.1. Quantum mechanics

QM calculations were carried out using the Gaussian 03 computer program [18]. Complete geometry optimizations were performed at the B3LYP [19,20] level combined with the 6-31G(d) basis set [21], *i.e.* B3LYP/6-31G(d). The minimum energy arrangements of 3T in both neutral and oxidized states were determined using a systematic conformational search strategy. For this purpose, the potential energy hypersurface of this compound was defined as $E = E(\theta,\theta')$, where θ and θ' refer to the flexible inter-ring dihedral angles (Scheme 2). The dihedral angles θ and θ' were scanned in steps of 30° between 0° and 360°, which led to build $12 \times 12 = 144$ structures. All these structures were calculated using a flexible rotor approximation. Thus, each structure was submitted to a constrained geometry optimization in which the inter-ring dihedral angles θ and θ' were kept fixed at the initial values.

The most stable arrangement of 3T was used to build up the 7T, which after complete geometry optimization was used to construct the 15T. The initial structures of 14T and 30T were obtained by dimerizing the optimized structures of 7T and 15T, respectively, the dihedral angle associated to such dimerization (θ_{D-D}) being initially arranged at 180°. It is worth noting that the lowest energy minimum

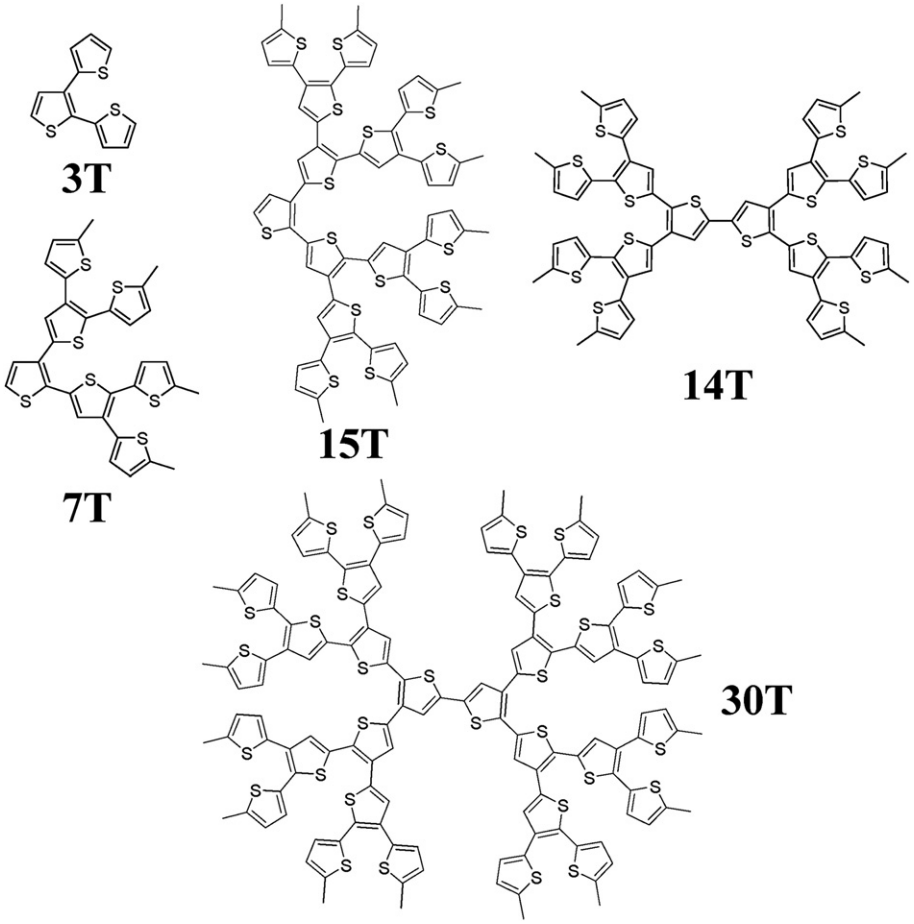

Scheme 1.

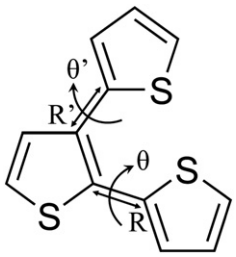

Scheme 2.

of α,α′-bithiophene corresponds to the *anti-gauche* ($\theta \cong 150^\circ$) and anti($\theta = 180^\circ$) conformations in the neutral [22] and oxidized [23] state, respectively. As was performed for 3T and 7T, the molecular geometries of 14T, 15T and 30T were optimized without any constraint. The structures of the dendrimers in the oxidized state, hereafter identified as $3T^+$, $7T^+$, $14T^+$, $15T^+$ and $30T^+$, was identical to that described for the systems in the neutral state. The restricted formalism was considered for calculations on neutral dendrimers (closed-shell systems), while for oxidized nT^+ systems the unrestricted formalism (UB3LYP) was used. For all the calculated dendrimers nT and nT^+, with exception of those with $n = 30$, frequency analyses were carried out to verify the nature of the minimum state of all the stationary points obtained by geometry optimization.

The lowest π–π^* transition energy (ε_g) in the neutral and oxidized states was obtained using two different strategies. In the first one, ε_g was estimated using the Koopman's theorem (KT) as the difference between the energies of the highest occupied molecular orbital (HOMO) and lowest unoccupied molecular orbital (LUMO) [24], *i.e.* $\varepsilon_g = \varepsilon_{LUMO} - \varepsilon_{HOMO}$. The second strategy consists on the evaluation of ε_g using time-dependent density functional theory (TD-DFT) [25]. More specifically, electronic excitations were evaluated at the (U)B3LYP/6-31G(d) level using the previously optimized geometries. On the other hand, the ionization potential of each dendrimer (IP) was estimated using the KT, that is, relating the IP to the energy of the HOMO [24]. However, more accurate IP values were obtained using the energies of the fully relaxed neutral and oxidized species. This approach, usually denoted ΔSCF, takes into account the relaxation energy of the ionized state, which can be calculated as the difference between KT and ΔSCF IPs [26,27].

2.2. Quantum mechanics/molecular mechanics

All QM/MM calculations were performed on $30T^+$ and 30T dendrimers assuming two ideal situations: (i) a dendrimer surrounded by four replicas placed in parallel stacking, *i.e.* sandwich arrangement; and (ii) a dendrimer surrounded by four replicas in T-shaped arrangement. Initially, these arrangements were built using the geometry of $30T^+$ optimized at the UB3LYP/6-31G(d) level. Accordingly, five dendrimers were involved in each supramolecular arrangement: 5·30T and $(5\cdot30T)^+$. The sandwich and T-shaped arrangements of $(5\cdot30T)^+$ were submitted to constrained geometry optimizations using MM, in which the intermolecular parameters were the only allowed to vary, *i.e.* the molecular geometry of $30T^+$ was kept fixed in all cases. MM minimizations were performed using the NAMD computer package [28]. The optimized geometries were used for single point QM/MM calculations of both the oxidized $(5\cdot30T)^+$ and the corresponding neutral system, *i.e.* 5·30T, which allowed to describe a complete redox process. In these calculations, which were carried out using the Gaussian 03 computer program [18], the central molecule was described at the (U)B3LYP/6-31G(d) QM level while the four surrounding replicas were represented as simple point charges. The molecular electrostatic potential (MEP) was computed at the (U)HF/6-31G(d) level for $30T^+$ and 30T. These calculations, which were performed on a large set of points located outside the nuclear region, were used to obtain the electrostatic charges applying an early developed procedure [29].

3. Results and discussion

3T has been considered as the building block of the nT with $n > 3$ dendrimers studied in the present work. Accordingly, a good description of this small compound becomes essential to build the rest of the dendrimers applying a bottom-up approach. Fig. 1 displays the potential energy hypersurfaces $E = E(\theta,\theta')$ calculated for 3T and $3T^+$ at the (U)B3LYP/6-31G(d). The global minimum of the neutral system appears at $\theta,\theta' = 125.2^\circ, -37.9^\circ$ (Fig. 2a), which upon

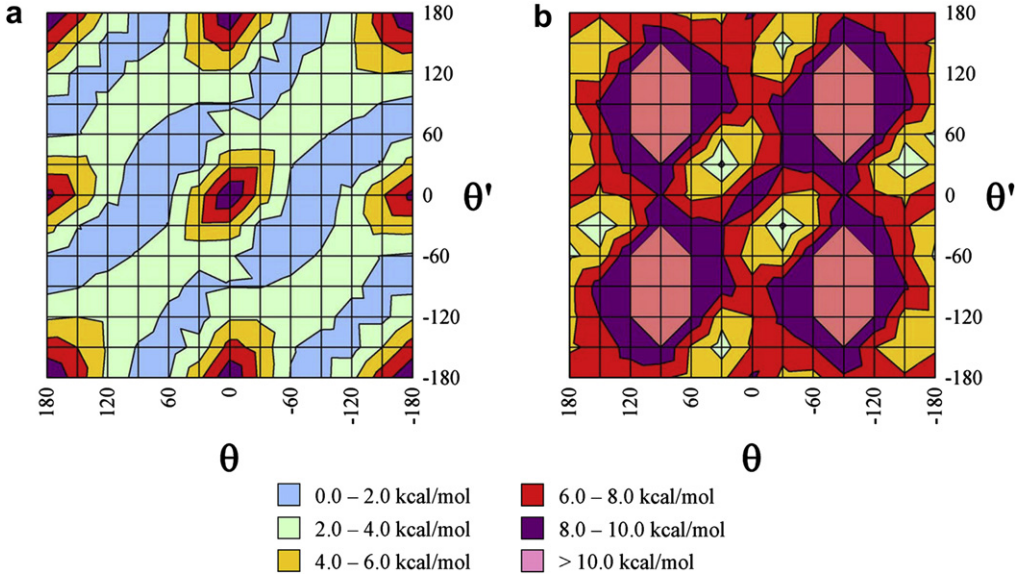

Fig. 1. Potential energy hypersurface $E = E(\theta,\theta')$ of (a) 3T and (b) $3T^+$ computed at the (U)B3LYP/6-31G(d) level.

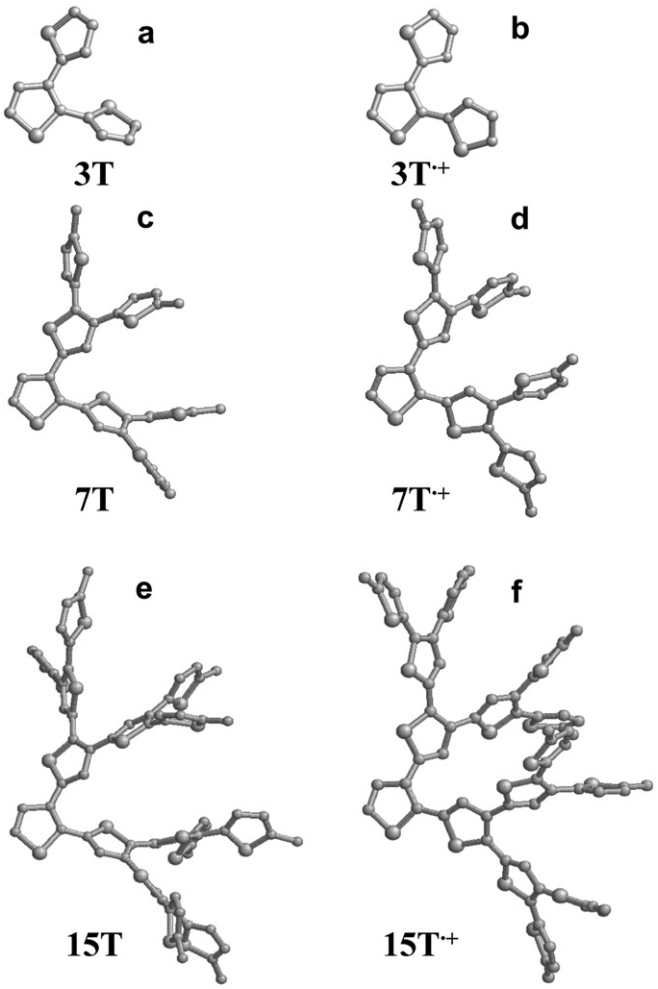

Fig. 2. Optimized structures of (a) 3T, (b) $3T^+$, (c) 7T, (d) $7T^+$, (e) 15T and (f) $15T^+$ calculated at the (U)B3LYP/6-31G(d) level. Hydrogen atoms have been omitted for clarity.

oxidation moves towards $\theta,\theta' = 26.6°, 28.1°$ (Fig. 2b). Comparison of the two hypersurfaces reveals that the rotational freedom is significantly higher for 3T than for $3T^+$. It is worth noting that planar conformations of the neutral building block, *i.e.* those with θ and θ' taking values of 0° or 180°, are severely destabilized (by more than 10 kcal/mol), which must be attributed to steric hindrance between the first and third thiophene rings. For $3T^+$ rotations around the α–α' and α'–β' linkages are clearly disfavored, which leads to a very rigid structure. This behavior is due to the formation of a quinoid structure in the oxidized specie that is clearly evidenced by the shortening of the inter-ring lengths, *e.g.* $R = 1.457/1.422$ Å and $R' = 1.466/1.432$ Å for the lowest energy minimum of $3T/3T^+$. Thus, rotation around a double bond involves a high energy penalty.

Table 1
Geometric parameters[a] for *n*T (with $n = 3$, 7 and 15) dendrimers in the neutral (plain text) and oxidized (*italic text*) states obtained from complete geometry optimizations at the (U)B3LYP/6-31G(d) level.

	θ (°)	θ' (°)	R (Å)	R'(Å)
3T	125.2	−37.9	1.457	1.466
	26.6	*28.1*	*1.422*	*1.432*
7T[b]	128.6 ± 1.2	-38.5 ± 0.7	$1.458 \pm 1.5 \times 10^{-3}$	$1.466 \pm 1.5 \times 10^{-3}$
	25.4 ± 3.0	*35.0 ± 5.6*	*1.435 ± 5.8 × 10⁻⁴*	*1.455 ± 8.7 × 10⁻⁴*
15T[c]	129.6 ± 1.4	-40.1 ± 0.6	$1.457 \pm 2.1 \times 10^{-3}$	$1.465 \pm 1.3 \times 10^{-3}$
	29.9 ± 4.0	*38.4 ± 2.6*	*1.445 ± 4.5 × 10⁻³*	*1.462 ± 3.8 × 10⁻³*

[a] See Scheme 2.
[b] Averages over the three values measured for each geometric parameter.
[c] Averages over the seven values measured for each geometric parameter.

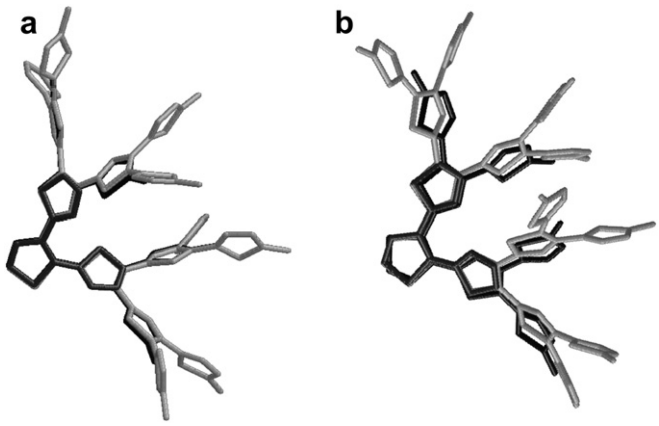

Fig. 3. Superposition of the optimized structures of: (a) 3T (dark gray), 7T (black) and 15T (light gray); and (b) $3T^+$ (dark gray), $7T^+$ (black) and $15T^+$ (light gray). Hydrogen atoms have been omitted for clarity.

The optimized structures of 3T and $3T^+$ were used as a building blocks to construct the third generation dendrimers, 7T and $7T^+$, respectively. Similarly, the optimized geometries of 7T and $7T^+$, which are displayed in Fig. 2c and d, were used to build 15T and $15T^+$, respectively. The structures obtained for these fourth generation dendrimers after complete geometry optimization are displayed in Fig. 2e and f, respectively. Average values for the dihedral angles θ and θ' as well as for the inter-ring bond lengths R and R' (see Scheme 2) for the neutral and oxidized dendrimers are reported in Table 1. As can be seen, the geometrical parameters predicted for 3T, 7T and 15T are very similar suggesting a regular growing pattern. Thus these three dendrimers are fully superimposable, as shown in Fig. 3a. On the other hand, oxidized dendrimers undergo substantial

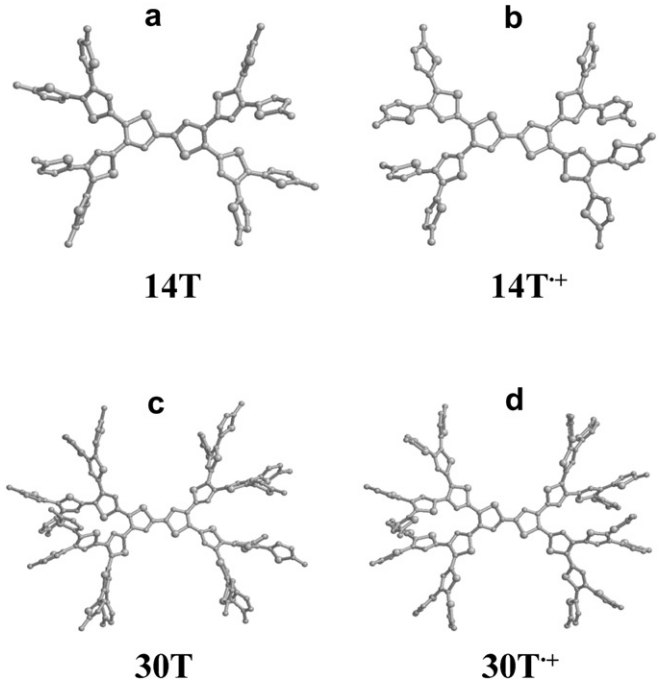

Fig. 4. Optimized structures of (a) 14T, (b) $14T^+$, (c) 30T and (d) $30T^+$ calculated at the (U)B3LYP/6-31G(d) level. Hydrogen atoms have been omitted for clarity.

Table 2
Geometric parameters[a,b] for *n*T (with $n = 14$ and 30) dendrimers in the neutral (plain text) and oxidized (*italic text*) states obtained from complete geometry optimizations at the (U)B3LYP/6-31G(d) level.

	θ (°)	θ' (°)	R (Å)	R'(Å)	θ_{D-D} (°)
14T[c]	131.5 ± 2.8	-40.6 ± 2.2	$1.455 \pm 1.4 \times 10^{-3}$	$1.466 \pm 1.9 \times 10^{-3}$	167.2
	28.2 ± 4.8	*39.8 ± 2.4*	*1.443 ± 7.5 × 10⁻³*	*1.464 ± 3.9 × 10⁻³*	*167.0*
30T[d]	131.5 ± 2.7	-40.8 ± 1.9	$1.456 \pm 1.9 \times 10^{-3}$	$1.466 \pm 1.5 \times 10^{-3}$	162.3
	33.6 ± 5.2	*40.1 ± 1.7*	*1.449 ± 5.4 × 10⁻³*	*1.466 ± 3.0 × 10⁻³*	*168.4*

[a] See Scheme 2.
[b] The inter-dendron dihedral angle has been defined by the S-C-C-S sequence.
[c] Averages over the six values measured for each geometric parameter.
[d] Averages over the fourteen values measured for each geometric parameter.

deviation from ideality, which increase with the molecular size. In spite of this behavior, that is mainly due to steric hindrance between neighboring sulfur atoms, Fig. 3b shows that the structures of the three oxidized dendrimers can be also superposed. It is also noticeable that the average inter-ring length R is slightly larger than that found in 2,2′,5′,2″-terthiophene, in which the two inter-ring linkages are α–α′, at the same level of theory (1.448 Å). This feature is consequence of both the steric hindrance between neighboring thiophene rings and the different distribution of charges (see Supporting Information). Comparison between the inter-ring bond lengths predicted for *n*T and $n\mathrm{T}^{+}$ reveals that, as expected, the differences (ΔR and $\Delta R'$) decreases with n, *e.g.* $\Delta R/\Delta R' = 0.035/0.034$ Å for $n = 3$ and $\Delta R/\Delta R' = 0.012/0.003$ Å for $n = 15$.

Fig. 4 shows the optimized structures of dendrimers 14T and 30T in both neutral and oxidized states, which were built upon *trans* α–α′ dimerization of dendrimers 7T and 15T, respectively. Inspection of the most relevant averaged geometric parameters for the neutral dendrimers (Table 2) shows a complete agreement with those of the parent structures 7T and 15T. However, steric hindrance caused again structural deviations from ideality in $14\mathrm{T}^{+}$ and $30\mathrm{T}^{+}$ leading to an increase up to 2.1% in the interthiophene bond R'. The inter-dendron dihedral angle, θ_{D-D} in Table 2, in the neutral dendrimers deviates slightly from 158.3° (8.9° and 4.0° for 14T and 30T, respectively), which is the inter-ring dihedral angle associated to the rotation of the α–α′ linkage in 2,2′-bithiophene predicted at the same level of theory. On the contrary, in $14\mathrm{T}^{+}$ and $30\mathrm{T}^{+}$ both steric hindrance and charge distribution lead to loss the planar structure, which is the most stable arrangement in oxidized 2,2′-bithiophene.

The IPs predicted by the KT and ΔSCF approaches for all the calculated dendrimers, which have been normalized considering an average per thiophene ring, are reported in Table 3. IPs predicted by the KT are slightly higher than those predicted by the ΔSCF, this difference being attributed to the fact that the latter approach takes into account the molecular relaxation of the ionized state. Both KT and ΔSCF IPs indicate that the energy needed to oxidize *n*T dendrimers decrease when n grows, which must be attributed to the increase of the electron delocalization with the molecular size. The same behavior was found in linear α-oligothiophenes [30]. Similarly, the IPs calculated for 14T and 30T are lower than those of their parent monomers, 7T and 15T, respectively.

Table 3
IPs calculated using the KT and ΔSCF approaches for dendrimers 3T, 7T, 15T, 14T and 30T. In order to facilitate the comparison, values have been normalized by considering the average per thiophene ring.

KT (eV ring^{-1})		ΔSCF (eV ring^{-1})	
3T	3.21	3T	2.26
7T	1.08	7T	0.84
14T	0.48	14T	0.39
15T	0.44	15T	0.37
30T	0.20	30T	0.18

Table 4
Lowest π–π* transition energy (ε_g; in eV) of *n*T and $n\mathrm{T}^{+}$ dendrimers obtained using the KT and TD-DFT methodologies at the (U)B3LYP/6-31G(d) level. Experimental values for the neutral systems, which were obtained using spectroscopy and oxidation–reduction potentials (in parenthesis for 14T and 30T), have been included for comparison. n_α refers to the longest α-conjugated chain of a given dendrimer.

	n_α	Neutral			Oxidized	
		KT	TD-DFT	Exp.[a]	KT	TD-DFT
3T	2	4.13	3.66	3.33	1.55	1.25
7T	3	3.51	3.05	2.82	0.84	0.80
15T	4	3.24	2.82	2.62	0.71	0.62
14T	6	2.95	2.60	2.48 (2.46)	0.54	0.43
30T	8	2.86	2.51	2.50 (2.51)	0.34	0.34

[a] Data from Ref. [5b]. Methyl groups have been used as terminators in this work, while hexyl groups were used in Ref. [5b].

The ε_g values estimated for *n*T and $n\mathrm{T}^{+}$ dendrimers using both the KT and TD-DFT calculations, in which HOMO–LUMO excitations are considered, are listed in Table 4, available experimental data [5b] being also included for comparison. In all cases the values estimated using the KT are overestimated with respect to the TD-DFT values. Comparison between the TD-DFT ε_g values and the experimental ones, which are available for the neutral dendrimers, reveal an excellent agreement. Furthermore, this notable concordance, that is especially remarkable for 14T and 30T dimers, increases with the molecular size. This indicates that the electronic structure of the neutral dendrimers is satisfactorily described by the TD-B3LYP/6-31G(d) methodology.

Fig. 5 represents the variation of the ε_g calculated at the TD-B3LYP/6-31G(d) for both *n*T and $n\mathrm{T}^{+}$ against $1/n_\alpha$, where n_α corresponds to the longest α-conjugated chain present of a given dendrimer. Additionally, available experimental data for *n*T [5b], as well as the ε_g values for linear α-oligothiophenes determined theoretically applying the KT [31] to the B3LYP/6-31G(d) energies and experimentally from the onset of the longest wavelength absorption band [6], are also plotted in Fig. 5 for comparison. In all cases, the ε_g decreases when the size of the α-conjugated chain increases. It should be noted that the overestimation of the ε_g values estimated for α-oligothiophenes using the KT with respect to the experimental values decreases with the molecular size, this behavior being also detected in *n*T dendrimers. In the latter systems, this should be attributed to the loss of planarity induced by the high branching. Comparison of the two experimental sets confirms this assumption for the two dimers, 14T and 30T. A linear

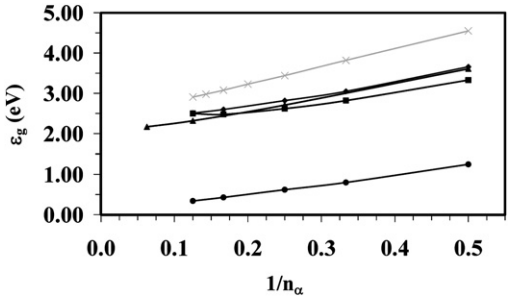

Fig. 5. Evolution of the π–π* lowest transition energy (ε_g; in eV) plotted against the inverse number of the longest α-conjugated chain present in each dendrimer ($1/n_\alpha$). The color and symbol codes correspond to: (i) ε_g calculated using the TD-B3LYP/6-31G(d) method for *n*T (diamonds); (ii) ε_g calculated using the TD-B3LYP/6-31G(d) method for $n\mathrm{T}^{+}$ (circles); (iii) experimental ε_g values (taken from reference [5b]) for $n\mathrm{T}^{+}$ (squares); (iv) ε_g calculated using the KT at the B3LYP/6-31G(d) level (taken from reference [27]) for linear α-oligothiophenes in the neutral state (crosses); and (v) experimental ε_g values (taken from reference [6]) for linear α-oligothiophenes in the neutral state (triangles).

regression analysis ($\varepsilon_g = a \cdot 1/n_\alpha + b$) using the ε_g predicted by TD-DFT calculations for neutral dendrimers was performed to extrapolate the value of an idealized dendrimer containing infinite thiophene units. The result, $\varepsilon_g = 2.08$ eV, indicates a reduction of 1.58 eV with respect to the value obtained for 3T. Regarding $n\mathrm{T}^+$, ε_g also shows a clear linear dependence with $1/n_\alpha$ (Fig. 5). As it can be seen, the ε_g predicted for oxidized dendrimers is significantly smaller than that of the neutral ones indicating the good performance of these systems as electronic conductors upon oxidation. This feature is especially remarkable for $30\mathrm{T}^{\cdot+}$, which shows a ε_g value that is 7.4 times smaller than that of 30T.

Given the aforementioned promising electronic properties of $n\mathrm{T}^+$ dendrimers, the modeling of their supramolecular assemblies is very desirable. For this purpose, calculations were performed on the largest oxidized dendrimer, *i.e.* $30\mathrm{T}^+$, which is the paradigmatic case. Specifically, we considered the stacked, also denoted sandwich, and T-shaped ideal arrangements of five molecules, $(5\cdot 30\mathrm{T})^+$, where a central dendrimer was surrounded by four replicas placed with coplanar and perpendicular orientations, respectively. The optimized geometry of the individual dendrimers was used to construct the assemblies. Figs. 6a and 7a depict the sandwich and T-shaped assemblies of $(5\cdot 30\mathrm{T})^+$, respectively, after energy minimization using MM. Due to both the lack of planarity and the large dimensions of $30\mathrm{T}^+$, the relative orientation between pairs of thiophene rings located at neighboring dendrimers is mainly perpendicular. This detail is illustrated in Figs. 6b and 7b for the sandwich and T-shaped supramolecular structures, respectively.

The geometries displayed in Figs. 6 and 7 were used to carry out single point QM/MM calculations not only of the oxidized system $(5\cdot 30\mathrm{T})^+$ but also of the neutral one, $5\cdot 30\mathrm{T}$, as was described in Methods. It is worth noting that, as we calculated the energy difference between the neutral and oxidized states of the part described using QM, both the MM and the QM/MM van der Waals contributions vanish because the geometries used for the two electronic states were identical. Thus, the only term that was not

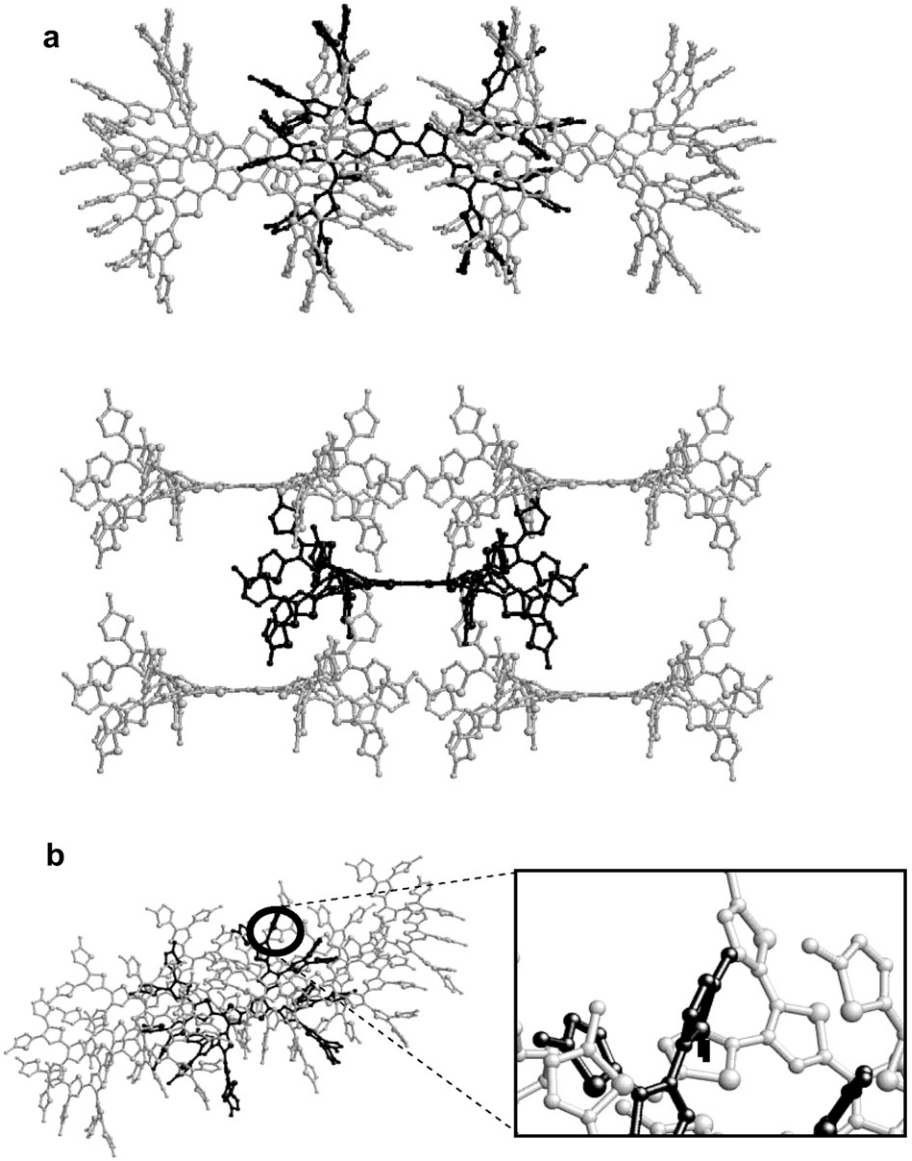

Fig. 6. Sandwich structure of $(5\cdot 30\mathrm{T})^{\cdot+}$: (a) equatorial (top) and axial (bottom) projections after energy minimization using MM; and (b) view of the stacking (indicated by a black line in the magnified picture) of the thiophene rings located at neighboring dendrimers. The dendrimer placed in the center is depicted in dark gray. Hydrogen atoms have been removed for clarity.

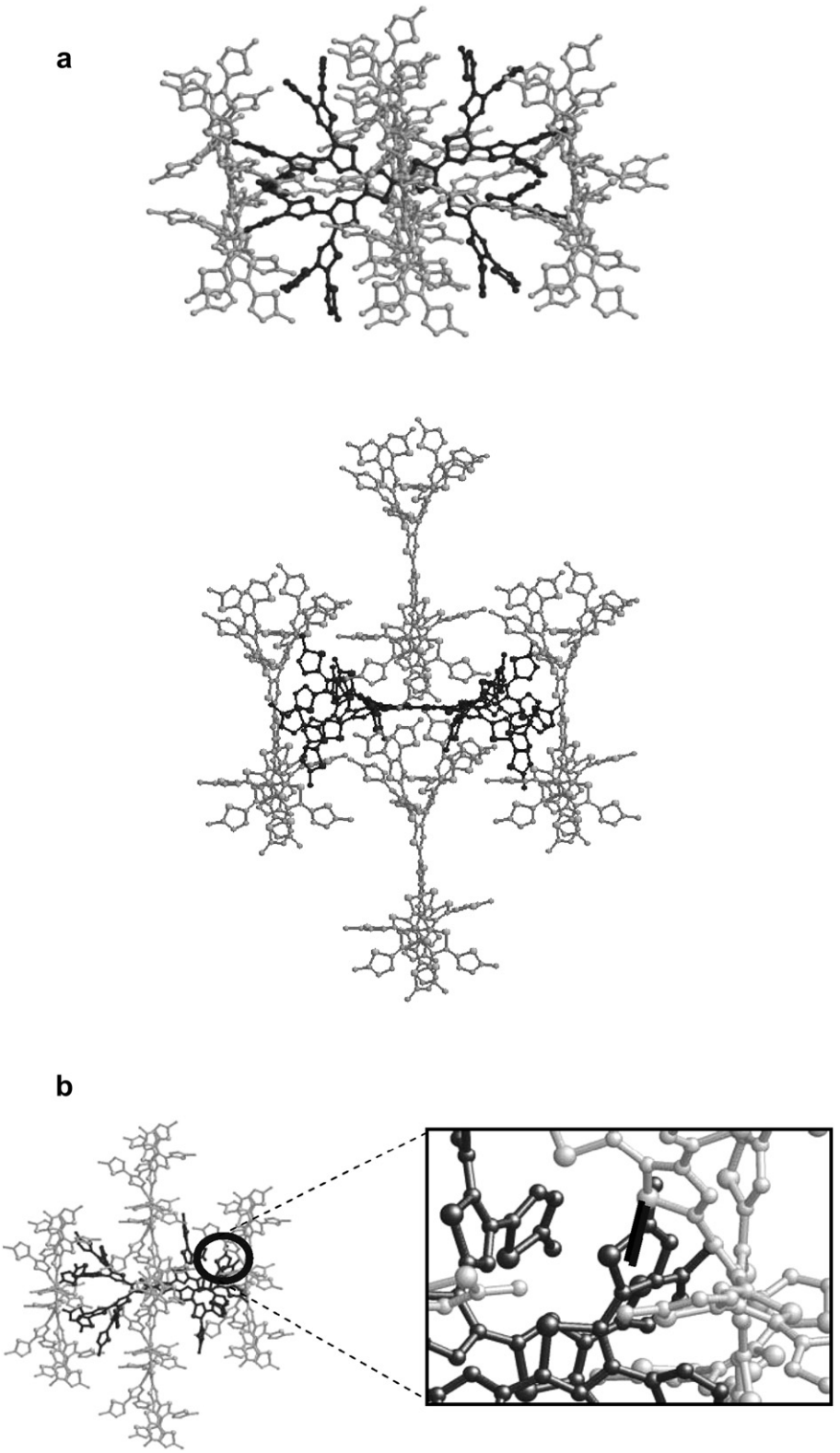

Fig. 7. T-shaped structure of $(5{\cdot}30T)^{\cdot+}$: (a) equatorial (top) and axial (bottom) projections after energy minimization using MM; and (b) view of the stacking (indicated by a black line in the magnified picture) of the thiophene rings located at neighboring dendrimers. The dendrimer placed in the center is depicted in dark gray. Hydrogen atoms have been removed for clarity.

canceled in such energy difference, apart from the QM energy, corresponds to the QM/MM electrostatic interaction since the polarization of the wave-function is a non-linear process [32]. Results obtained from these calculations are summarized in Table 5. As can be seen, the two arrangements show similar ε_g and IP values, the most noticeable result being the reduction of ε_g for the neutral system with respect to the isolated dendrimer. Thus, the ε_g predicted for 30T using the KT was 2.86 eV (Table 4), whereas the value

Table 5
Ionization potential (IP) and lowest π–π^* transition energy ($\varepsilon_{g,neutral}$) of 5·30T and lowest π–π^* transition energy ($\varepsilon_{g,oxidized}$) of $(5\cdot30T)^+$ derived from QM/MM calculations considering the sandwich and T-shaped arrangements. In order to facilitate the comparison, the IP values have been normalized by considering the average per thiophene ring.

	IP (eV ring^{-1})	$\varepsilon_{g,neutral}$ (eV)	$\varepsilon_{g,oxidized}$ (eV)
Sandwich	0.17	2.32	0.32
T-Shaped	0.16	2.33	0.32

of this property decreases to 2.32–2.33 eV, depending on the supramolecular arrangement, when the intermolecular electronic delocalization is allowed. Thus, thiophene–thiophene stacking interactions promote this intermolecular phenomenon, which is added to the intrinsic intramolecular electronic delocalization, narrowing the energy difference between HOMO and LUMO, *i.e.* reducing the ε_g [33].

Accordingly, QM/MM calculations confirm the ability of the investigated dendrimers to form aggregates and their good performance when assembled in supramolecular arrangements. Thus, they should be considered as novel conducting polymers with potential electrooptical applications. On the other hand, it should be noted that, if longer alkyl chains are used as terminal groups (in the present paper we have used methyl as terminal groups), only the T-shaped arrangement is no possible due to the steric hindrances. Moreover, longer alkyl groups would stabilize the overall sandwich arrangement because of the favorable van der Waals interactions between neighboring molecules.

4. Conclusions

QM calculations have been used to get an accurate description of the molecular and electronic structure of a series of all-thiophene dendrimers in both the neutral and oxidized states. Independently of the electronic state, minimum energy structures were found to present repulsive steric interactions between the neighboring thiophene rings, which induce significant distortions from the coplanarity of thiophene rings. Within this context, the regular growing pattern of neutral dendrimers is especially remarkable since it favors the formation of highly regular architectures. On the other hand, the highest generation dendrimers exhibited the lowest IP per ring, which is consequence of the largest electron delocalization. Moreover, ε_g values derived from TD-DFT calculations, which were in excellent agreement with available experimental data for very similar all-thiophene dendrimers, presented a reciprocal interdependence with the inverse of the longest α-conjugated chain of the dendrimer, *i.e.* ε_g decreases when the generation increases. Extrapolation of the results derived from TD-DFT calculations in the neutral dendrimers allowed predict a ε_g value of 2.08 eV for an idealized infinite generation dendrimer. Oxidized dendrimers presented very small ε_g values suggesting that they behave as excellent electronic conductors upon p-doping.

QM/MM calculations on systems formed by five dendrimers reflected the ability of these materials to form supramolecular aggregates in both sandwich and T-shaped arrangements, the latter being only feasible when short chains are used as terminators. Furthermore, these calculations have evidenced the influence of the intermolecular electronic delocalization, which reduces considerably the ε_g. The overall of these results offers a deeper insight on the electronic structure that controls the electrooptical properties characteristic of all-thiophene dendrimers and indicates that they are a very promising family of conducting materials.

Acknowledgements

This work has been supported by MCYT and FEDER (Grants MAT2006-04029 and MAT2009-09138), and by the Generalitat de Catalunya (Grants 2009-SGR-925 and XRQTC). Authors are indebted to the "Centre de Supercomputació de Catalunya" (CESCA) for the computational resources provided. F.R.R. thanks the FPU program for financial support of the MEC. D.Z. thanks financial support from the Ramon y Cajal program of the Spanish "Ministerio de Educación y Ciencia" (MEC). Support for the research of C.A. was received through the prize "ICREA Academia" for excellence in research funded by the Generalitat de Catalunya.

Appendix. Supplementary data

Atomic coordinates and absolute energies of the *n*T and $n\text{T}^+$ minima as well as the he electrostatic charges of 30T and 30T^+ are available in the supporting information. Supplementary data associated with this article can be found in the online version, at doi:10.1016/j.polymer.2009.11.007.

References

[1] (a) Otero TF, Sariñena JM. Adv Mater 1998;10:491–4;
(b) Dai L, Winkler B, Dong L, Tong L, Mau AWH. Adv Mater 2001;13:915–25;
(c) Tour JM. Acc Chem Res 2000;33:791–804.
[2] Roncali J. Chem Rev 1992;92:711–38.
[3] Chan HSO, Ng SC. Prog Polym Sci 1998;23:1167–231.
[4] Mishra A, Ma CQ, Bäuerle P. Chem Rev 2009;109:1141–276.
[5] (a) Xia C, Fan X, Locklin J, Advincula RC. Org Lett 2002;4:2067–70;
(b) Xia C, Fan X, Locklin J, Advincula RC, Gies A, Nonidez W. J Am Chem Soc 2004;126:8735–43.
[6] Ma CQ, Mena-Osteritz E, Debaerdemaeker T, Wienk MM, Janssen RAJ, Bäuerle P. Angew Chem Int Ed 2007;46:1679–83.
[7] Ramakrishna G, Bhaskar A, Bäuerle P, Goodson III T. J Phys Chem A 2008;112:2018–26.
[8] Benincori T, Capaccio M, De Angelis F, Falciola L, Muccini M, Mussini P, et al. Chem Eur J 2008;14:459–71.
[9] Harpham MR, Süzer Ö, Ma CQ, Bäuerle P, Goodson III T. J Am Chem Soc 2009;131:973–9.
[10] (a) Bosman AW, Janssen HM, Meijer EW. Chem Rev 1999;99:1665;
(b) Zhang A. Prog Chem 2005;17:157–71;
(c) Frauenrath H. Prog Polym Sci 2005;30:325–84;
(d) Schlüter AD. Top Curr Chem 2005;245:151–91;
(e) Schlüter AD, Rabe JP. Angew Chem Int Ed 2000;39:864–83;
(f) Ballauff M, Likos CN. Angew Chem Int Ed 2004;43:2998–3020.
[11] Jang WD, Selim KMK, Lee CH, Kang IK. Prog Polym Sci 2009;34:1–23.
[12] Caminade AM, Servin P, Laurent R, Majoral JP. Chem Soc Rev 2008;37:56–67.
[13] Astruc D, Ornelas C, Ruiz J. Acc Chem Res 2008;41:841–56.
[14] Percec V, Glodde M, Bera TK, Miura Y, Shiyanovskaya I, Singer KD, et al. Nature 2002;419:384–7.
[15] (a) Percec V, Ahn CH, Ungar G, Yeardley DJP, Möller M, Sheiko SS. Nature 1998;391:161–4;
(b) Percec V, Imam MR, Peterca M, Wilson DA, Heiney PA. J Am Chem Soc 2009;131:1294–304.
[16] Sonar P, Benmansour H, Geiger T, Schlüter AD. Polymer 2007;48:4996–5004.
[17] Graf DD, Campbell JP, Miller LL, Mann KR. J Am Chem Soc 1996;118:5480–1.
[18] Frisch MJ, Trucks GW, Schlegel HB, Scusseria GE, Robb MA, Cheeseman JR, et al. Gaussian 03: revision B.02. Pittsburgh, PA: Gaussian, Inc.; 2003.
[19] Becke AD. J Chem Phys 1993;98:1372–7.
[20] Lee C, Yang W, Parr RG. Phys Rev B 1988;37:785–9.
[21] Hariharan PC, Pople JA. Theor Chim Acta 1973;28:213–22.
[22] Rodríguez-Ropero F, Casanovas J, Alemán C. Chem Phys Lett 2005;416:331–5.
[23] Casanovas J, Alemán C. J Phys Chem C 2007;111:4823–30.
[24] Koopmans T. Physica 1934;1:104–13.
[25] Runge E, Gross EKU. Phys Rev Lett 1984;52:997–1000.
[26] Casanovas J, Ricart JM, Rubio J, Illas F, Jiménez-Mateos JM. J Am Chem Soc 1996;118:8071–6.
[27] Casanovas J, Alemán C. J Phys Chem A 2004;108:1440–7.
[28] Phillips JC, Braun R, Wang W, Gumbart J, Tajkhorshid E, Villa E, et al. J Comput Chem 2005;26:1781–802.
[29] Alemán C, Casanovas J. J Chem Soc Perkin Trans 1994;2:563–8.
[30] Johansson E, Larsson S. Synth Met 2004;144:183–91.
[31] Alemán C, Armelin E, Iribarren JI, Liesa F, Laso M, Casanovas J. Synth Met 2005;149:151–6.
[32] Jacquemin D, Perpète EA, Laurent AD, Assfeld X, Adamo C. Phys Chem Chem Phys 2009;11:1258–62.
[33] Rodríguez-Ropero F, Casanovas J, Alemán CJ. Comput Chem 2007;29:69–78.